

DARK HALO AND DISK GALAXY SCALING LAWS IN HIERARCHICAL UNIVERSES

JULIO F. NAVARRO¹

Department of Physics and Astronomy, University of Victoria, Victoria, BC V8P 1A1, Canada

AND

MATTHIAS STEINMETZ²

Steward Observatory, University of Arizona, Tucson, AZ 85721, USA

Draft version October 27, 2018

ABSTRACT

We use cosmological N-body/gasdynamical simulations that include star formation and feedback to examine the proposal that scaling laws between the total luminosity, rotation speed, and angular momentum of disk galaxies reflect analogous correlations between the structural parameters of their surrounding dark matter halos. The numerical experiments follow the formation of galaxy-sized halos in two Cold Dark Matter dominated universes: the standard $\Omega = 1$ CDM scenario and the currently popular Λ CDM model. We find that the slope and scatter of the I-band Tully-Fisher relation are well reproduced in the simulations, although not, as proposed in recent work, as a result of the cosmological equivalence between halo mass and circular velocity: large systematic variations in the fraction of baryons that collapse to form galaxies and in the ratio between halo and disk circular velocities are observed in our numerical experiments. The Tully-Fisher slope and scatter are recovered in this model as a direct result of the dynamical response of the halo to the assembly of the luminous component of the galaxy. We conclude that models that neglect the self-gravity of the disk and its influence on the detailed structure of the halo cannot be used to derive meaningful estimates of the scatter or slope of the Tully-Fisher relation. Our models fail, however, to match the zero-point of the Tully-Fisher relation, as well as that of the relation linking disk rotation speed and angular momentum. These failures can be traced, respectively, to the excessive central concentration of dark halos formed in the Cold Dark Matter cosmogonies we explore and to the formation of galaxy disks as the final outcome of a sequence of merger events. Disappointingly, our feedback formulation, calibrated to reproduce the empirical correlations linking star formation rate and gas surface density established by Kennicutt, has little influence on these conclusions. Agreement between model and observations appears to demand substantial revision to the Cold Dark Matter scenario or to the manner in which baryons are thought to assemble and evolve into galaxies in hierarchical universes.

Subject headings: cosmology: theory – galaxies: formation, evolution – methods: numerical

1. INTRODUCTION

The structural parameters of dark matter halos formed in hierarchically clustering universes are tightly related through simple scaling laws that reflect the cosmological context of their formation. These correlations result from the approximately scalefree process of assembly of collisionless dark matter into collapsed, virialized systems. Analytical studies and cosmological N-body simulations have been particularly successful at unraveling the relations between halo mass, size, and angular momentum, as well as the dependence of these correlations on the cosmological parameters. The picture that emerges is encouraging in its simplicity and in its potential applicability to the origin of scaling laws relating the structural properties of galaxy systems (see, e.g., Dalcanton, Spergel & Summers 1997, Mo, Mao & White 1998 and references therein).

One example is the relation between halo mass and size—a direct result of the finite age of the universe. The nature of this correlation and its dependence on the cosmological parameters is straightforward to compute using simple spherical collapse models of “top-hat” density pertur-

bations that have been found to be in good agreement with the results of numerical experiments (see, e.g., Cole & Lacey 1996, Eke, Cole & Frenk 1996, Eke, Navarro & Frenk 1998, and references therein).

A second example concerns the angular momentum of dark halos, which is also linked to halo mass and size through simple scaling arguments. Expressed in nondimensional form, the angular momentum of dark matter halos is approximately independent of mass, environment, and cosmological parameters, a remarkable result likely due to the scalefree properties of the early tidal torques between neighboring systems responsible for the spin of individual halos (Peebles 1969, White 1984, Barnes & Efstathiou 1988, Steinmetz & Bartelmann 1995).

Finally, similarities in the halo formation process are also apparent in the internal structure of dark halos. A number of numerical studies have consistently shown that the shape of the density profiles of dark halos is approximately “universal”; i.e., it can be well approximated by a simple two-parameter function whose formulation is approximately independent of mass, redshift, and cosmology

¹CIAR Scholar, Alfred P. Sloan Fellow. Email: jfn@uvic.ca

²Alfred P. Sloan Fellow, David & Lucile Packard Fellow. Email: msteinmetz@as.arizona.edu

(Navarro, Frenk & White 1996, 1997, hereafter NFW96 and NFW97, respectively; Cole & Lacey 1996; Tormen, Bouchet & White 1996, Huss, Jain & Steinmetz 1999a,b).

How do these scaling properties relate to analogous correlations between structural parameters of disk galaxy systems? This paper is third in a series where this question is addressed through direct numerical simulation of galaxy formation in cold dark matter (CDM) dominated universes. In spirit, these studies are similar to those of Evrard, Summers & Davis 1994, Tissera, Lambas & Abadi 1997, Elizondo et al. 1999, although are conclusions differ in detail from those reached by them. The first paper in our series (Steinmetz & Navarro 1999, hereafter SN1) examined the origin of the Tully-Fisher relation under the assumption that star formation is dictated by the rate at which gas cools and collapses within dark halos. We were able to show that the velocity scaling of luminosity and angular momentum in spiral galaxies arise naturally in hierarchical galaxy formation models.

Large discrepancies, however, were observed in the zero point of these correlations, a result we ascribed to the early dissipative collapse of gas into the progenitor dark matter halos and to the subsequent assembly of the final system through a sequence of mergers (Navarro & Benz 1991, Navarro, Frenk & White 1995, Navarro & Steinmetz 1997, hereafter NS97). We concluded then, in agreement with a number of previous studies, that agreement between models and observations requires a large injection of energy (presumably “feedback” energy from evolving stars and supernovae) in order to prevent much of the gas from cooling and condensing into (proto)galaxies at early times, shifting the bulk of star formation to later times and alleviating the angular momentum losses associated with major mergers (White & Rees 1978, White & Frenk 1991, Kauffmann, White & Guiderdoni 1993, Cole et al. 1994).

This hypothesis remains to date the most attractive path to resolve the “disk angular momentum problem”. On the other hand, further analysis has shown that the zero-point offset between the model and observed Tully-Fisher relations is actually due to the high central concentrations of dark matter halos formed in currently popular versions of the Cold Dark Matter cosmogony, and therefore is unlikely to be reconciled through feedback effects (Navarro & Steinmetz 2000, hereafter NS2). We investigate these issues in detail in the present paper, which represents our first attempt at implementing a realistic numerical formulation of feedback within a full-fledged simulation of the formation of galaxies in CDM halos, and at gauging its effects on the origin of disk galaxy scaling laws.

The paper is organized as follows. Section 2 motivates our approach by reviewing the scaling laws linking the properties of dark matter halos and by comparing them with observational correlations. A brief description of the numerical procedure is included in §3; full details of the star formation, feedback prescription, and relevant tests will be presented in Steinmetz & Navarro (2000, hereafter SN3). Section 4 discusses our main results regarding the slope, scatter and zero-point of the Tully-Fisher relation and of the relation between disk angular momentum and rotation speed. We summarize and discuss our main re-

sults in §5, and conclude in §6.

2. DARK HALO AND DISK GALAXY SCALING LAWS

2.1. Mass, Radius, and Circular Velocity

The radial distribution of mass in dark halos has no obvious edge, so defining halo “sizes” is a somewhat arbitrary procedure. A plausible and useful choice is to associate the radius of a halo with the distance from the center at which mass shells are infalling for the first time. This “virial radius” is easily estimated from N-body simulations and imposes, by construction, a firm upper limit to the mass of the galaxy embedded inside each halo: baryons beyond the virial radius have not had time yet to reach the center of the halo and therefore cannot have been accreted by the central galaxy.

Numerical experiments show that virial radii depend sensitively on the enclosed mass of the system, in a way consistent with the predictions of the spherical top-hat collapse model. The “edge” of a halo occurs approximately where the mean inner density contrast, Δ , is of order a few hundred.³ This result seems to apply equally well to halos of all masses, and depends only weakly on cosmology through the density parameter, Ω , and the cosmological constant, Λ , (Eke et al. 1996, 1998),

$$\Delta(\Omega, \Lambda) \approx 178 \begin{cases} \Omega^{0.30}, & \text{if } \Lambda = 0; \\ \Omega^{0.45}, & \text{if } \Omega + \Lambda = 1. \end{cases} \quad (1)$$

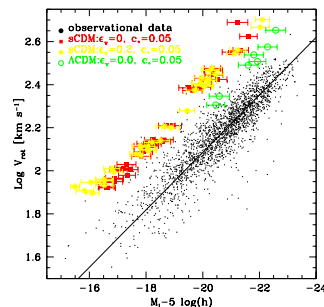


FIG. 1.—The I-band Tully-Fisher relation compared with the results of the numerical simulations. Dots correspond to the observational samples of Mathewson, Ford & Buchhorn, (1992), Giovanelli et al (1997), Willick et al (1997), and Han & Mould (1992). Error bars in the simulated magnitudes correspond to adopting a Salpeter or a Scalo IMF.

One consequence of this definition is that all halos identified at a given time have similar densities, from where it follows on dimensional grounds that the total mass of the halo and its circular velocity at the virial radius must be tightly related. In terms of the circular velocity, V_Δ , at the virial radius, r_Δ , halo masses are given by

$$M_\Delta(V_\Delta, z) = \left(\frac{2}{\Delta}\right)^{1/2} \frac{V_\Delta^3}{GH(z)} = 1.9 \times 10^{12} \left(\frac{\Delta}{200}\right)^{-1/2} \times \frac{H_0}{H(z)} \left(\frac{V_\Delta}{200 \text{ km s}^{-1}}\right)^3 h^{-1} M_\odot. \quad (2)$$

³We use the term “density contrast” to refer to densities expressed in units of the critical density for closure, $\rho_{crit} = 3H(z)^2/8\pi G$, where $H(z)$ is the value of Hubble’s constant at redshift z . We parameterize the present value of H as $H_0 = H(z=0) = 100 h \text{ km s}^{-1} \text{ Mpc}^{-1}$.

This power-law dependence on velocity is similar to that of the I-band Tully-Fisher relation linking the luminosity and rotation speed of late-type spirals,

$$L_I \approx 2.0 \times 10^{10} \left(\frac{V_{\text{rot}}}{200 \text{ km s}^{-1}} \right)^3 h^{-2} L_{\odot}, \quad (3)$$

(see solid line in Figure 1) a coincidence that suggests a direct cosmological origin for this scaling law. Eqs. 2 and 3 can be combined to read,

$$L_I = 1.9 \times 10^{12} \frac{1}{\Upsilon_I} \frac{M_{\text{disk}}}{M_{\Delta}} \frac{H_0}{H(z)} \left(\frac{\Delta}{200} \right)^{-1/2} \left(\frac{V_{\Delta}}{V_{\text{rot}}} \right)^3 \times \left(\frac{V_{\text{rot}}}{200 \text{ km s}^{-1}} \right)^3 h^{-1} L_{\odot}, \quad (4)$$

where we have introduced the parameter M_{disk} to represent the total mass associated with the galaxy disk and $\Upsilon_I = M_{\text{disk}}/L_I$ is the disk mass-to-light ratio in solar units⁴

Combining eqs. 2, 3, and 4, we find that the fraction of the total mass of the system in the galaxy disk is, at $z = 0$,

$$f_{\text{mdsk}} = \frac{M_{\text{disk}}}{M_{\Delta}} = 8.5 \times 10^{-3} h^{-1} \left(\frac{\Delta}{200} \right)^{1/2} \Upsilon_I \left(\frac{V_{\text{rot}}}{V_{\Delta}} \right)^3. \quad (5)$$

This result reemphasizes our implicit assumption that within the “virial radius” galaxy systems are dominated by dark matter. Further insight can be gained by comparing M_{disk} to the total baryonic mass within r_{Δ} , $M_{\text{disk}}^{\text{max}} = (\Omega_b/\Omega_0)M_{\Delta}$. Assuming that the baryon density parameter is $\Omega_b \approx 0.0125 h^{-2}$, as suggested by Big Bang nucleosynthesis studies of the primordial abundance of the light elements (Schramm & Turner 1997), the fraction of baryons transformed into stars in disk galaxies is given by,

$$f_{\text{bdsk}} = \frac{M_{\text{disk}}}{M_{\text{disk}}^{\text{max}}} \approx 0.85 \Omega_0 h \Upsilon_I \left(\frac{\Delta}{200} \right)^{1/2} \left(\frac{V_{\text{rot}}}{V_{\Delta}} \right)^3. \quad (6)$$

Because by definition baryons outside the virial radius have yet to reach the galaxy, $M_{\text{disk}}^{\text{max}}$ is a firm upper bound to the baryonic fraction transformed into stars, implying that $f_{\text{bdsk}} \lesssim 1$ (White et al. 1993).

The slope and zero point of the Tully-Fisher relation therefore implies that the fraction of the total mass (and of baryons) transformed into stars is a sensitive function of the cosmological parameters (through the product $\Omega_0 h$, and Δ), of the stellar mass-to-light ratio, and of the ratio between the rotation speed of the disk and the circular velocity of the surrounding halo.

2.1.1. Constraints from the slope of the Tully-Fisher relation

⁴Note that this definition of the disk mass-to-light ratio includes stellar and gaseous mass. However, most of the baryons in the Tully-Fisher disks we consider here are actually in stars (this is true for observed as well as for simulated galaxies) so that the stellar and “baryonic” disk mass-to-light ratio differ very little. We shall not discriminate between them throughout this paper. Further, we assume $M_I(\odot) = 4.15$ for all numerical values quoted in this paper.

⁵According to these authors, the density profile of a dark halo is well approximated by $\rho(r) = \delta_c \rho_{\text{crit}} (r/r_s)^{-1} (1 + r/r_s)^{-2}$, where r_s is a scale radius and δ_c is a characteristic density contrast. For halos of given mass, M_{Δ} , this formula has a single free parameter, which can be expressed as the “concentration”, $c = r_{\Delta}/r_s$. The characteristic density contrast and the concentration are related by the simple formula, $\delta_c = (\Delta/3) c^3 / (\ln(1+c) - c/(1+c))$.

As indicated by eq. 5, reproducing the observed slope of the Tully-Fisher relation entails a delicate balance between f_{mdsk} , Υ_I , and the ratio $V_{\text{rot}}/V_{\Delta}$. The simplest possibility is that the three parameters are approximately constant in all halos. This is the case argued by Mo et al. (1998), who suggest that $f_{\text{mdsk}} \approx 5 \times 10^{-2}$, $\Upsilon_I \approx 1.7 h$, and $V_{\text{rot}}/V_{\Delta} \approx 1.5$ are needed in order to reproduce observations of galaxy disks. Although plausible, this assumption is at odds with the results of the numerical experiments we present below (§3), so it is worthwhile considering a second possibility: that f_{mdsk} , Υ_I , and $V_{\text{rot}}/V_{\Delta}$ are not constant from halo to halo but that their variations are strongly correlated, in the manner prescribed by eq. 5. We explore now how such correlation may emerge as a result of the dynamical response of the dark halo to the assembly of a disk galaxy at its center.

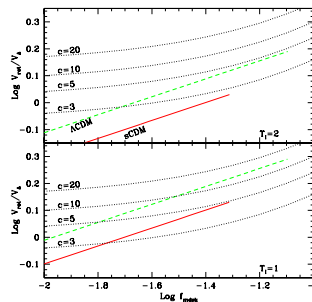


FIG. 2.—The disk mass fraction versus the ratio between disk rotation speed and halo circular velocity. The thick dashed and solid lines correspond to the *constraint* imposed on these two quantities by the Tully-Fisher relation (eq. 5) in the Λ CDM and SCDM scenarios, respectively. Dotted lines correspond to the relation expected for galaxies assembled in NFW halos of constant “concentration” parameter, as labeled. Constant disk mass-to-light ratios are assumed throughout; $\Upsilon_I = 2$ in the upper panel and $\Upsilon_I = 1$ in the lower one, respectively.

In the interest of simplicity, we shall restrict our analysis to a case where the disk mass-to-light ratio, Υ_I , is assumed to be constant, and we shall use the “adiabatic contraction” approximation to compute the dependence of the velocity ratio $V_{\text{rot}}/V_{\Delta}$ on f_{mdsk} . The resulting relation is sensitive to the detailed mass profile of the dark halo and to the assumed structure of the disk. Assuming that the model proposed by Navarro, Frenk & White (NFW96, NFW97)⁵ is a reasonable approximation to the structure of the halo, and adopting exponential disk models with radial scale lengths consistent with the assumption that halo and disk share the same specific angular momentum, it is possible to derive analytically the dependence of the velocity ratio on f_{mdsk} (see Mo et al 1998 for details). We show the results in Figure 2. The thick lines (solid and dashed) in this figure correspond to the constraint enunciated in eq. 5 for two different cosmological models (the “standard” Cold Dark Matter model, sCDM: with parameters $\Omega = 1$ and $h = 0.5$, and a low-density, flat Λ CDM

model, with $\Omega_0 = 0.3$, $\Lambda_0 = 0.7$, and $h = 0.7$). The upper and lower panels adopt two different values for the disk mass-to-light ratio, $\Upsilon_I = 2$, and 1, respectively. The rightmost point in each of the thick lines corresponds to the maximum disk mass fraction allowed by the baryonic content of the halo, i.e., $f_{\text{mdsk}}^{\text{max}} = \Omega_b/\Omega_0$. Dotted lines in this figure are the “adiabatic contraction approximation” predictions for different values of the NFW concentration parameter, c .

Figure 2 illustrates a few interesting points. The first one is that the disk mass-to-light ratio and the cosmological parameters determine in practice the range of halo concentrations that are consistent with the zero-point of the Tully Fisher relation. Halos formed in the Λ CDM scenario must have $c \lesssim 3$ (5) if $\Upsilon_I \approx 2$ (1). This effectively rules out the Λ CDM scenario, since N-body simulations show that halos formed in this cosmology have much higher concentrations, typically $c \sim 15$ -20 (NFW96). A similar conclusion was reached by van den Bosch (1999), who finds through similar considerations that the large V_{rot}/V_Δ values expected in the Λ CDM scenario effectively rule out this cosmogony.

The low-density Λ CDM model fares better, because the higher value of h and the lower value of Δ in this model imply smaller f_{mdsk} at a given value of the velocity ratio V_{rot}/V_Δ . However, for $\Upsilon_I = 2$ (1), concentrations lower than about ~ 5 (12) are needed. As discussed by NS2, high-resolution N-body simulations of halo formation in the Λ CDM scenario yields concentrations of order ~ 20 , in disagreement with these constraints unless $\Upsilon_I \ll 1$. Concentrations as high as this are similar to those found for Λ CDM, and are systematically higher than the values predicted by the approximate formula proposed by NFW97. This explains the apparent disagreement between the conclusions of NS2 and those of semi-analytic models that claim reasonable agreement with the observed Tully-Fisher relation (Mo et al 1998, van den Bosch 1999): the discrepancy can be fully traced to the lower halo central concentrations and lower disk mass-to-light ratios adopted by the latter authors. If concentrations are truly as high as reported by NS2, agreement with the Tully Fisher relation require $\Upsilon_I \ll 1$, in disagreement with estimates based on broad-band colors of Tully-Fisher disks (which suggest $\Upsilon_I \approx 2$) and with mass-to-light ratio estimates of the solar neighborhood (see NS2 for details).

The second important point that emerges from Figure 2 is that, in order to match the Tully-Fisher relation, halo concentrations must be an increasing function of f_{mdsk} (assuming $\Upsilon_I \approx \text{constant}$). Indeed, as f_{mdsk} increases the thick solid and dashed lines cross (dotted) curves of increasing c . Since, according to NFW96 and NFW97, concentration depends directly on halo mass—low mass halos are systematically more centrally concentrated as a result of earlier collapse times—this is equivalent to requiring f_{mdsk} to be a function of halo mass. This is actually consistent with simple disk formation models where the mass of the disk is determined by gas cooling radiatively inside a dark halo, as first proposed by White & Rees (1978), and later worked out in detail by White & Frenk (1991). These authors show that, if disks form by gas cooling within an approximately isothermal halo, disk masses are expected to be roughly proportional to $V_\Delta^{3/2}$ (White 1996), imply-

ing $f_{\text{mdsk}} \propto V_\Delta^{-3/2} \propto M_\Delta^{-1/2}$. We show below (§4.1) that, although this dependence is stronger than found in our numerical experiments, the overall trend predicted is nicely reproduced in our numerical experiments.

Finally, Figure 2 illustrates that the structure and dynamical response of the halo to the assembly of the disk may be responsible for the small scatter in the Tully-Fisher relation. For illustration, consider two halos of the same mass, and therefore approximately similar concentration, where the fraction of baryons collected into the central galaxy, f_{mdsk} , differs substantially. Provided that $f_{\text{mdsk}} \gtrsim 0.02$, where the “adiabatic contraction” dotted curves are approximately parallel to the observational constraint delineated by the thick lines, these two galaxies will lie approximately along the same Tully-Fisher relation. Even if the concentration of the two halos were to differ greatly its effect on the scatter of the Tully-Fisher relation would be relatively minor: at fixed f_{mdsk} , V_{rot}/V_Δ changes by only about 20% when c changes by a factor of two.

To summarize, assuming that the disk mass-to-light ratio is approximately constant for Tully-Fisher disks, the slope of the I-band Tully-Fisher relation may result from the combination of three effects: (i) the reduced efficiency of cooling in more massive halos, (ii) the mass dependence of halo concentrations, and (iii) the dynamical response of the halo to the disk assembly. This also offers a natural explanation for the small scatter in the observed Tully-Fisher relation. We shall use our numerical simulations to test the verisimilitude of this speculation below.

2.2. Circular Velocity and Angular Momentum

Another similarity between the properties of dark halos and galaxy disks concerns their angular momentum. N-body simulations show that, in terms of the dimensionless parameter, $\lambda = J|E|^{1/2}/GM_\Delta^{5/2}$, the distribution of halo angular momenta is approximately independent of mass, redshift, and cosmological parameters, and may be approximated by a log-normal distribution peaked at around $\lambda \sim 0.05$ (Cole & Lacey 1996 and references therein). (J and E are the total angular momentum and binding energy of the halo, respectively.)

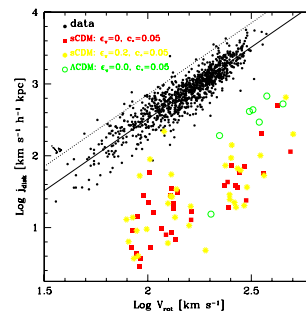


FIG. 3.—Specific angular momentum vs circular velocity of model galaxies compared with observational data. Data correspond to the samples of Courteau (1997), Mathewson et al (1992), and the compilation of Navarro (1999). Specific angular momenta are computed from disk scalelengths and rotation speeds, assuming an exponential disk model with a flat rotation curve.

The binding energy depends on the internal structure of

the halos but the structural similarity between dark halos established by NFW96 and NFW97 implies that E is to good approximation roughly proportional to $M_\Delta V_\Delta^2$, with a very weak dependence on the characteristic density of the halo. The specific angular momentum of the halo then may be written as (see Mo et al 1998 for further details),

$$j_\Delta \approx 2 \frac{\lambda}{\Delta^{1/2}} \frac{V_\Delta^2}{H(z)} = 2.8 \times 10^3 \frac{H_0}{H(z)} \left(\frac{\Delta}{200} \right)^{-1/2} \times \left(\frac{V_\Delta}{200 \text{ km s}^{-1}} \right)^2 \text{ km s}^{-1} h^{-1} \text{ kpc}, \quad (7)$$

where we have used the most probable value of $\lambda = 0.05$ in the second equality (see dotted line in Figure 3). The simple velocity-squared scaling of this relation is identical to that illustrated in Figure 3 between the specific angular momentum of disks and their rotation speed,

$$j_{\text{disk}} \approx 1.3 \times 10^3 \left(\frac{V_{\text{rot}}}{200 \text{ km s}^{-1}} \right)^2 \text{ km s}^{-1} h^{-1} \text{ kpc} \quad (8)$$

(solid line in Figure 3), suggestive, as in the case of the Tully-Fisher relation, of a cosmological origin for this scaling law.

Combining eqs. 7 and 8, we can express the ratio between disk and halo specific angular momenta at $z = 0$ as,

$$f_j = \frac{j_{\text{disk}}}{j_\Delta} \approx 0.45 \left(\frac{\Delta}{200} \right)^{1/2} \left(\frac{V_{\text{rot}}}{V_\Delta} \right)^2. \quad (9)$$

If the rotation speeds of galaxy disks are approximately the same as the circular velocity of their surrounding halos, then disks must have retained about one-half of the available angular momentum during their assembly.

The velocity ratio may be eliminated using eq. 6 to obtain a relation between the fraction of baryons assembled into the disk and the angular momentum ratio,

$$f_j \approx 0.5 \left(\frac{\Delta}{200} \right)^{1/6} \left(\frac{f_{\text{b,disk}}}{\Omega_0 h \Upsilon_I} \right)^{2/3}. \quad (10)$$

This combined constraint posed by the Tully-Fisher and the angular momentum-velocity relation is shown in Figure 4 for two different cosmological models. As in Figure 2, thick solid lines correspond to the “standard” cold dark matter model, sCDM, and thick dashed lines to the Λ CDM model. Each curve is labelled by the value adopted for the disk mass-to-light ratio, Υ_I . The precise values of $f_{\text{b,disk}}$ and f_j along each curve are determined by and the ratio V_{rot}/V_Δ , and are shown by starred symbols for the case $V_{\text{rot}} = V_\Delta$ and $\Upsilon_I = 1$.

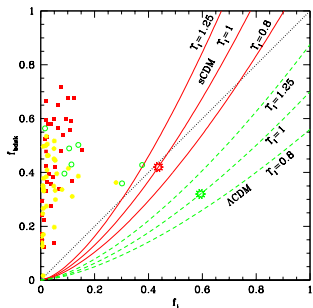


FIG. 4.—The fraction of the baryons assembled into a disk galaxy ($f_{\text{b,disk}}$) versus the ratio between the specific angular momenta of the disk and its surrounding halo (f_j). Thick solid and dashed lines correspond to the constraints imposed by the Tully-Fisher relation (Figure 1) and by the relation between rotation speed and angular momentum (Figure 3). The solid (dashed) thick line corresponds to the sCDM (Λ CDM) scenario, shown for different values of Υ_I , as labeled. Symbols correspond to simulated galaxy models as per the labels in Figure 1.

One important point illustrated by Figure 4 is that disk galaxies formed in a low-density universe, such as Λ CDM, need only accrete a small fraction of the total baryonic mass to match the zero-point of the Tully-Fisher relation, but must draw a much larger fraction of the available angular momentum to be consistent with the spins of spiral galaxies. For example, if $V_{\text{rot}} = V_\Delta$ and $\Upsilon_I = 1$, disk masses amount to only about 30% of the total baryonic mass of the halo but contain about 60% of the available angular momentum. This is intriguing and, at face value, counterintuitive. Angular momentum is typically concentrated in the outer regions of the system (see, e.g., Figure 9 in NS97), presumably the ones least likely to cool and be accreted into the disk, so it is puzzling that galaxies manage to tap a large fraction of the available angular momentum whilst collecting a small fraction of the total mass. The simulations in NS97, which include the presence of a strong photo-ionizing UV background, illustrate exactly this dilemma; the UV background suppresses the cooling of late-infalling, low-density, high-angular momentum gas and reduces the angular momentum of cold gaseous disks assembled at the center of dark matter halos.

The situation is less severe in high-density universes such as sCDM; we see from Figure 4 that disks are required to collect similar fractions of mass and of angular momentum in order to match simultaneously the Tully-Fisher and the spin-velocity relations. As a result, any difficulty matching the angular momentum of disk galaxies in sCDM will become only worse in a low-density Λ CDM universe.

Note as well that the problem becomes more severe the lower the mass-to-light ratio of the disk. Indeed, from the point of view of this constraint, it would be desirable for disks formed in the Λ CDM scenario to have $\Upsilon_I \gtrsim 2$; in this case $f_j \sim f_{\text{b,disk}}$ would be consistent with the constraint posed by observed scaling laws. However, this is the opposite of what was required to reconcile highly-concentrated halos with the zero-point of the Tully-Fisher relation. This conundrum illustrates the fact that accounting simultaneously for the mass and angular momentum of disk galaxies represents a serious challenge to hierarchical models of galaxy formation.

3. NUMERICAL EXPERIMENTS

3.1. The Code

The simulations were performed using GRAPESPH, a code that combines the hardware N-body integrator GRAPE with the Smooth Particle Hydrodynamics technique (Steinmetz 1996). GRAPESPH is fully Lagrangian and optimally suited to study the formation of highly non-linear systems in a cosmological context. The version used

here includes the self-gravity of gas, stars, and dark matter components, a three-dimensional treatment of the hydrodynamics of the gas, Compton and radiative cooling, the effects of a photo-ionizing UV background (NS97), and a simple recipe for transforming gas into stars.

3.2. The Star Formation and Feedback Algorithm

The numerical recipe for star formation, feedback and metal enrichment is similar to that described in Steinmetz & Müller (1994, 1995, see also Katz 1992, Navarro & White 1993). Full details on our present implementation are presented in Steinmetz & Navarro (2000), together with validating and calibrating tests. A brief description follows.

“Star particles” are created in collapsing regions that are locally Jeans unstable at a rate controlled by the local cooling and dynamical timescales, $\dot{\rho}_* = c_* \rho_{gas} / \max(\tau_{cool}, \tau_{dyn})$. The proportionality parameter, c_* , effectively controls the depletion timescale of gas, which in high-density regions, where most star formation takes place and where $\tau_{dyn} \gg \tau_{cool}$, is of order $\tau_{dyn}/c_* \approx (4\pi G \rho_{gas})^{-1/2} c_*^{-1}$.

The equations of motion of star particles are only affected by gravitational forces, but newly formed stars devolve $\sim 10^{49}$ ergs (per solar mass of stars formed) about 10^7 yrs after their formation. This energy input, a crude approximation to the energetic feedback from evolving massive stars and supernovae, is largely invested in raising the temperature of the surrounding gas. As discussed by Katz (1992) and Navarro & White (1993), this form of energetic feedback is rather inefficient; the high densities typical of star forming regions imply short cooling timescales that minimize the hydrodynamical effects of the feedback energy input. The net result is that the star formation history of an object simulated using this “minimal feedback” formulation traces closely the rate at which gas cools and collapses within dark matter halos (SN1).

We have generalized this formulation by assuming that certain fraction of the available energy, ϵ_v , is invested in modifying the kinetic energy of the surrounding gas. These motions can still be dissipated through shocks but on longer timescales, leading to overall reduced star formation efficiencies and longer effective timescales for the conversion of gas into stars.

We have determined plausible values for the two parameters, c_* and ϵ_v , by comparing the star forming properties of isolated disk galaxy models with the empirical “Schmidt-law” correlations between star formation rate and gas surface density reported by Kennicutt (1998, see SN3 for full details). In the case of “minimal feedback” ($\epsilon_v = 0$) low values of c_* , typically ~ 0.05 , are needed to prevent the rapid transformation of all of the gas in a typical galaxy disk into stars. Introducing a kinetic component to the feedback prolongs the depletion timescales somewhat, but in all cases, best results are obtained by choosing long star formation timescales, i.e., values of $c_* \sim 0.05$. For such low values of c_* , ϵ_v must be less than 0.2 in order to prevent slowing down star formation to rates significantly lower than observed in Kennicutt’s empirical correlations. Similar constraints on ϵ_v can be derived from high resolution 1D simulations of supernova remnants (Thorn-ton et al. 1998). We shall hereafter refer to the (rather extreme) choice of $c_* = 0.05$ and $\epsilon_v = 0.2$ as the “kinetic feedback” case. Adopting $c_* > 0.05$ and $\epsilon_v < 0.2$

produces results that are intermediate between the “minimal” and “kinetic” feedback cases we report here. Tests on isolated disks of varying circular velocity indicate that the “kinetic feedback” adopted here reduces substantially the efficiency of star formation in systems with circular velocity below ~ 100 km s $^{-1}$, but has a more modest influence on the star formation rates in more massive systems, in rough agreement with current interpretation of observational data (Martin 1999).

3.3. The Initial Conditions

We investigate two variants of the Cold Dark Matter scenario. The first is the former “standard” CDM model, with cosmological parameters $\Omega = 1$, $h = 0.5$, $\Lambda = 0$, normalized so that at $z = 0$ the rms amplitude of mass fluctuations in $8h^{-1}$ Mpc spheres is $\sigma_8 = 0.63$. Although this model fails to reproduce a number of key observations, such as the CMB fluctuations detected by COBE, it remains popular as a well-specified cosmological testbed and as a well studied example of a hierarchical clustering model of galaxy formation. The second is the currently popular low-density CDM model that includes a non-zero cosmological constant and which is normalized to match COBE constraints and current estimates of the Hubble constant, $\Omega_0 = 0.3$, $\Lambda = 0.7$, $h = 0.7$, $\sigma_8 = 1.1$. Both models assume a value of $\Omega_b = 0.0125 h^{-2}$ for the baryon density parameter of the universe, consistent with constraints from Big-Bang nucleosynthesis of the light elements (Schramm & Turner 1997).

In both cosmologies, we simulate regions that evolve to form dark halos with circular velocities in the range (80, 350) km s $^{-1}$ at $z = 0$. These regions are selected from cosmological simulations of large periodic boxes and are resimulated individually including the full tidal field of the original calculation. All resimulations have typically 32,000 gas particles and the same amount of dark matter particles. The size of the resimulated region scales with the circular velocity of the selected halo, so that most systems have similar numbers of particles at $z = 0$, regardless of circular velocity. This is important to ensure that numerical resolution is approximately uniform across all systems. Gas particle masses range from $2.5 \times 10^6 h^{-1} M_\odot$ to $9 \times 10^7 h^{-1} M_\odot$, depending on the system being simulated. Dark matter particle masses are a factor $(\Omega_0 - \Omega_b)/\Omega_b$ more massive. Their mass is low enough to prevent artificial suppression of cooling due to collisional effects (Steinmetz & White 1997). Runs start at $z = 21$ and use gravitational softenings that range between 0.5 and $1.0 h^{-1}$ kpc.

We have concentrated our numerical efforts on the sCDM scenario: about 60 galaxy models satisfy the conditions for analysis outlined below (§3.4). For comparison, only seven Λ CDM galaxy models are considered here. This is because of our realization during the course of this study that the cosmological scenario has very modest effects on the scaling laws we discuss here. Indeed, regarding disk scaling laws, galaxy models formed in the sCDM and Λ CDM scenarios differ mainly because of the adoption of different values of the Hubble constant. We discuss this in more detail below.

3.4. Identification and Analysis of Model Galaxies

Model galaxies are easily identified in our runs as star and gas “clumps” with very high density contrast. We

retain for analysis only galaxies in halos represented with more than 500 dark particles inside the virial radius; most of these systems have more than 1,000 star particles in each galaxy. This list is culled to remove obvious ongoing mergers and satellites orbiting the main central galaxy of each halo. The properties of the luminous component are computed within a fiducial radius, $r_{gal} = 15 (V_{\Delta}/220 \text{ km s}^{-1}) h^{-1} \text{ kpc}$. This radius contains all of the baryonic material associated with the galaxy and is much larger than the spatial resolution of the simulations. The rotation speeds we quote are also measured at that radius, although in practice the circular velocity in the models is rather insensitive to the radius where it is measured: similar results are obtained using $r_{gal} = 3.5 (V_{\Delta}/220 \text{ km s}^{-1}) h^{-1} \text{ kpc}$ (see Figure 1 of SN1).

Although the resolution of the modeled galaxies is adequate to compute reliably quantities such as the total mass or circular velocity as a function of radius, it is still insufficient to gain insight into the morphology of the galaxy. As a result, our sample is likely to contain a mixture of Hubble types, from S0 to Sd (most of the simulated galaxies retained for analysis are largely rotationally supported).

Galaxy luminosities are computed by simply adding the luminosities of each star particle, taking into account the time of creation of each particle and using the latest version of the spectrophotometric models of Bruzual & Charlot (G. Bruzual & S. Charlot 1996, unpublished), see Conrardo, Steinmetz & Fritze-von Alvensleben (1998) for details. Corrections due to internal absorption and inclination are neglected. The IMF is assumed in all cases to be independent of time.

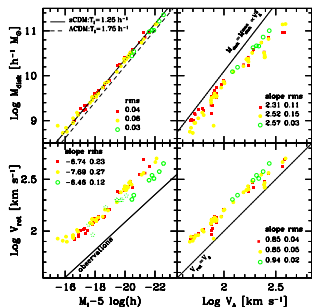


FIG. 5.—Correlations between disk mass, M_{disk} , disk rotation speed (measured at r_{gal}), V_{rot} , absolute I-band magnitude at $z = 0$, M_I , and halo circular velocity, V_{Δ} , found in the numerical experiments. Symbols are as in Figure 1. Solid line in the lower-left panel is the best fit to the observational data shown in Figure 1. Solid and dashed lines in the upper left panel correspond to constant disk mass-to-light ratio, $\Upsilon_I = 2.5$. Solid line in upper-right panel outline the loci of galaxies that have assembled all available baryons. Slopes quoted in all panels correspond to unweighted least-squares fits. The rms scatter values correspond to the y -axis quantity relative to the least-squares fit, except for the M_I - V_{rot} panel, where it corresponds to the scatter in M_I .

4. NUMERICAL SCALING LAWS

4.1. The numerical Tully-Fisher relation

The symbols with horizontal error bars in Figure 1 show the numerical Tully-Fisher relation obtained in our simulations. Solid squares and open circles denote the luminosities and rotation speeds (measured at r_{gal}) of galaxy models formed in the sCDM and Λ CDM scenarios, respectively, under the “minimal feedback” assumption. Starred symbols correspond to the “kinetic feedback” case applied to the sCDM model. Error bars span the range in luminosities corresponding to assuming either a Salpeter or a Scalo stellar initial mass function.

A few points are clear from Figure 1. (i) The scatter and slope of the numerical Tully-Fisher relation are in good agreement with observation. (ii) The zero point of the numerical relation is offset by almost 2 (1.25) magnitudes for sCDM (Λ CDM) galaxy models. (iii) The effects of kinetic feedback on the numerical Tully-Fisher relation are quite modest. Indeed, only a slight dimming in galaxies with $V_{\text{rot}} \lesssim 100 \text{ km s}^{-1}$ is clearly noticeable in Figure 1. We analyze these three results in detail below.

4.1.1. The Slope

As discussed in §2.1, agreement between the slopes of the numerical and observed I-band Tully-Fisher relation imply a tight relation between the fraction of the mass assembled into the galaxy, f_{mdsk} , the disk mass-to-light ratio, Υ_I , and the ratio between disk and halo circular velocities, $V_{\text{rot}}/V_{\Delta}$ (see eq. 5). Correlations between these parameters obtained in our numerical simulations are shown in Figure 5.

The bottom left panel of Figure 5 is identical to Figure 1, but labels includes the (unweighted) best-fit slope and rms deviation (in magnitudes) of each numerical relation. Symbols are as in Figure 1. As mentioned above, the slopes of the sCDM relations are consistent with the observed one. The same applies to the Λ CDM best-fit slope, which is virtually indistinguishable from the sCDM one. This result is only weakly affected by the narrow dynamic range covered by the Λ CDM simulations. Indeed, extending our analysis to more poorly resolved clumps in the Λ CDM runs (systems with $V_{\text{rot}} < 200 \text{ km s}^{-1}$, see dotted open circles in this panel) shows that there is little significant difference between the effective slopes obtained in the sCDM and Λ CDM models (see also Figure 2 of NS2). The good agreement between observed and numerical slopes indicate that f_{mdsk} , Υ_I , and $V_{\text{rot}}/V_{\Delta}$ approximately follow the constraint prescribed by eq. 5. The rest of the panels in Figure 5 illustrate the nature of this relation.

The upper left panel in Figure 5 shows that, to a large extent, the stellar mass-to-light ratios of galaxy models are approximately constant; the dotted and dashed lines in this panel correspond to $\Upsilon_I = 2.5 = \text{constant}$. On the other hand, the disk mass fraction is far from constant from system to system. As illustrated by the upper right panel in Figure 5, baryons in low circular velocity halos are much more effective at condensing into central galaxies than those in more massive systems. Indeed, as V_{Δ} increases, the numerical results move away from the solid line representing galaxies which have assembled *all* of the available baryons.⁶ The fraction of baryons assembled into the central galaxy varies from $\sim 70\%$ in halos with

⁶The symbols corresponding to the Λ CDM model (open circles) have been rescaled downwards in the upper right panel of Figure 5 so that the $M_{\text{disk}} = M_{\text{disk}}^{\text{max}}$ solid line is the same as in sCDM. Vertical deviations from this solid line thus indicate in both cases variations in the fraction of baryons assembled into the central galaxy.

$V_{\Delta} \lesssim 100 \text{ km s}^{-1}$ to less than $\sim 20\%$ in $V_{\Delta} \sim 300 \text{ km s}^{-1}$ halos. This result is unlikely to be an artifact of limited numerical resolution since, as discussed in §3.3, the numerical resolution of the simulations do not depend systematically on halo circular velocity. Furthermore, the same trend was found in the convergence study of Navarro & Steinmetz (NS97, see their Table 1); the observed trend between f_{mdsk} and V_{Δ} must therefore reflect the decreasing efficiency of gas cooling in halos of increasing mass discussed in §2.1.1.

In spite of the large systematic variations in the disk mass fraction put in evidence by Figure 5, the numerical slope of the Tully-Fisher relation is in good accord with observations because f_{mdsk} variations are compensated by corresponding changes in the $V_{\text{rot}}/V_{\Delta}$ ratio. Low mass halos have higher f_{mdsk} values, but also higher $V_{\text{rot}}/V_{\Delta}$ ratios than more massive ones (bottom right panel of Figure 5). For constant Υ_I , agreement with the observed TF slope requires $f_{\text{mdsk}} = M_{\text{disk}}/M_{\Delta} \propto M_{\text{disk}}/V_{\Delta}^3 \propto (V_{\text{rot}}/V_{\Delta})^3$ (see eq. 5), so that if $M_{\text{disk}} \propto V_{\Delta}^{\alpha}$, then $V_{\text{rot}} \propto V_{\Delta}^{\alpha/3}$ must be satisfied. Inspection of the exponents (“slopes”) listed in the right-hand panels of Figure 5 demonstrate that this condition is approximately satisfied in the numerical experiments.

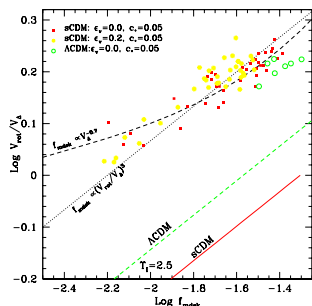


FIG. 6.—As in Figure 2, but including the results of the numerical simulations. The dotted line shows the proportionality $f_{\text{mdsk}} \propto (V_{\text{rot}}/V_{\Delta})^3$. The thick dashed line shows the “adiabatic contraction” prediction assuming that a $f_{\text{mdsk}} \propto V_{\Delta}^{-0.7}$, and that the NFW concentration parameter is given by $c = 20(V_{\Delta}/100 \text{ km s}^{-1})^{-1/3}$, as found in the numerical experiments. See text for further details.

Figure 6 illustrates this conclusion more explicitly: the numerical results follow very closely the $f_{\text{mdsk}} \propto (V_{\text{rot}}/V_{\Delta})^3$ proportionality outlined by the dotted line. As discussed in §2.1.1, this proportionality results from the combination of three effects: (i) the decreasing disk mass fraction in halos of increasing mass ($f_{\text{mdsk}} \propto V_{\Delta}^{-0.7}$ approximately, see upper-right panel of Figure 5), (ii) the decrease in concentration of halos of increasing mass ($c \approx 20(V_{\Delta}/100 \text{ km s}^{-1})^{-1/3}$, see NFW96 and NS2), and (iii) the response of the dark halo to the assembly of the disk. The thick dashed line in Figure 6 shows the f_{mdsk} vs. $(V_{\text{rot}}/V_{\Delta})$ relation that results from these three premises using the adiabatic contraction approximation described in §2.1.1; it clearly reproduces the numerical results remarkably well.

We conclude that the agreement between the slopes of the numerical and observed Tully-Fisher relations lends support to the view that the Tully-Fisher slope is the (non-trivial) result of the combined effects of the halo structure

and of its response to the assembly of the baryonic component of the galaxy.

4.1.2. The Zero Point

In contrast with the good agreement found between models and observations for the Tully-Fisher slope, it is clear from Figure 1 that there is a serious mismatch in the zero-point of the numerical and observed Tully-Fisher relations. This is reflected in Figure 6 as a systematic offset between the numerical data points and the thick curves labeled “sCDM” and “ Λ CDM” (analogous to the lines in Figure 2, but drawn here for $\Upsilon_I = 2.5$, as appropriate for our numerical results). At given f_{mdsk} , the ratio $V_{\text{rot}}/V_{\Delta}$ is much larger than required by observations, leading to galaxies which, at fixed rotation speed, are too faint to be consistent with observations, as clearly shown in Figure 1. Simulated galaxies formed in the sCDM and Λ CDM scenarios are physically very similar, since they have similar disk mass-to-light ratios and share the same location in the f_{disk} vs. $(V_{\text{rot}}/V_{\Delta})$ plane. The reason why Λ CDM models appear to be in better agreement with observations in Figure 1 is largely due to the adoption of a higher value of Hubble’s constant for this model. This issue is discussed in detail by NS2. From the analysis in that paper and the discussion in §2.1.1, it is clear that the zero-point discrepancy is testimony to the large central concentrations of dark halos formed in the two cosmologies we explore here.

4.1.3. The Scatter

According to eq. 4, the scatter in the numerical Tully-Fisher relation is determined by the variance in the mass-to-light ratio, Υ_I , the disk mass fraction, f_{mdsk} , and the velocity ratio, $V_{\text{rot}}/V_{\Delta}$. These can be derived from the rms values quoted in the right-hand panels and upper-left panel of Figure 5, respectively, and would imply, taken at face value, a large dispersion ($\gtrsim 0.6 \text{ mag rms}$) for the numerical Tully-Fisher relation. This is actually about *three times* larger than measured in the simulations (see rms values quoted in bottom left panel of Figure 5). The reason behind the small scatter is once again linked to the dynamical response of the halo to the disk assembly, as discussed in §2.1.1. At fixed halo mass (i.e., fixed V_{Δ}), galaxies where fewer than average baryons collect into the central galaxy have lower than average $V_{\text{rot}}/V_{\Delta}$ ratios, and vice-versa. This is shown in Figure 7, where we plot the residuals from the best-fit power laws to the data presented in the right-hand panels of Figure 5. As anticipated in §2.1.1, the residuals scale in such a way that variations in the fraction of baryons assembled into galaxies scatter *along* the observed Tully-Fisher relation, reducing substantially the resulting scatter. This helps to reconcile the large scatter predicted by analytical estimates (Eisenstein & Loeb 1996) with the results of our numerical simulations. Again, the halo structure and response to the assembly of the galaxy are crucial for explaining the observed properties of the Tully-Fisher relation.

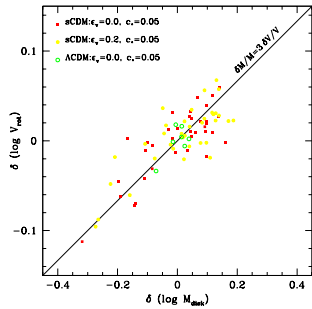


FIG. 7.—Residuals from least squares fits to the numerical data presented in the right-hand panels of Figure 5. Solid line corresponds to the condition $\delta \log M_{\text{disk}} = 3 \delta \log V_{\text{rot}}$ required so that galaxy models scatter *along* the Tully-Fisher relation, reducing substantially its scatter.

4.2. The angular momentum of simulated disks

In agreement with prior work (see, e.g., NS97 and references therein), we find that the baryonic components of the simulated galaxy models are quite deficient in angular momentum. This is easily appreciated in Figure 3, which shows that, at a given V_{rot} , the specific angular momentum of observed disks exceeds that of numerical models by more than one order of magnitude. This is due to the transfer of angular momentum from the baryons to the halo associated with merger events during the formation of the disk, as first suggested by Navarro & Benz (1991), and later confirmed by Navarro, Frenk & White (1995) and NS97. Indeed, as shown in Figure 4, the baryonic components of simulated galaxies have retained, on average, less than 15% of the specific angular momentum of their surrounding halos, placing them in the $(f_{\text{b,disk}}, f_j)$ plane well outside of the constraints imposed by the observed scaling laws between luminosity, rotation speed, and disk size.

4.3. The effects of feedback

Our implementation of feedback seems to have only a very modest impact on the results discussed above, even for the rather extreme “kinetic feedback” case we tried. In the case of the Tully-Fisher relation only systems with $V_{\text{rot}} \lesssim 100 \text{ km s}^{-1}$ are affected (see, e.g., starred symbols in Figure 1), and the net effect is actually to make the zero-point disagreement worse: the rotation speeds of these low-mass galaxies are roughly unchanged, but feedback makes them fainter. This shows yet again that the zero-point problem afflicting the Tully-Fisher relation is not a result of processes that affect the baryonic component, such as feedback, but of the high central concentration of dark matter near the centers of dark halos and the relatively high disk mass-to-light ratios of our models.

Feedback also seems to have a relatively minor impact on the “angular momentum problem” as well. Disks simulated with our “minimum” and “kinetic” feedback implementations have angular momenta well below those of observed spirals (Figures 3 and 4). Feedback seems able to slow down the transformation of gas into stars in low-mass systems but fails to prevent most of the gas from collapsing into dense disks at early times. The final galaxy is thus built up as the outcome of a hierarchical sequence of merger events during which the gas transfers most of its angular momentum to its surrounding halo (NS97 and references therein).

We conclude that the feedback algorithm explored here is unable to bring the angular momenta of simulated galaxies into agreement with observations. Gas must be effectively prevented from collapsing into, or removed from, dense disks at early times, a requirement that requires a much more efficient transformation of supernova energy into gas bulk motions than our algorithm can accomplish (Weil, Eke & Efstathiou 1998). However, it is difficult to see how this can be attained without violating constraints posed by observed correlations between gas density and star formation rates in isolated disks (Kennicutt 1998). As discussed in §3.2, the “kinetic feedback” model parameters adopted here are already quite extreme; for example, increasing ϵ_v beyond our choice of 20% in an effort to expel more gas from star forming regions would lead to models that disagree substantially with Kennicutt’s findings (SN3). Although it cannot be discounted that feedback implementations different from the one adopted here may lead to improved results, we conclude that accounting simultaneously for the luminosity, velocity, and angular momentum of spiral galaxies in hierarchical models remains an unsolved problem for the CDM cosmogonies we explore here.

5. SUMMARY AND DISCUSSION

We report here the results of numerical experiments designed to explore whether cosmologically induced correlations linking the structural parameters of cold dark matter halos may serve to elucidate the origin of disk galaxy scaling laws. The numerical experiments include gravity, pressure gradients, hydrodynamical shocks, radiative cooling, heating by a UV background, and a simple recipe for star formation. Feedback from evolving stars is also taken into account by injecting energy into gas that surrounds regions of recent star formation. A large fraction of the energy input is in the form of heat, and is radiated away quickly by the dense, cool, star-forming gas. The remainder is introduced through an extra acceleration term that affects directly the kinematics of the gas in the vicinity of star forming regions.

We find that the slope of the numerical Tully-Fisher relation is in good agreement with observation, although not, as proposed in previous work, as a direct result of the cosmological equivalence between mass and circular velocity of dark halos. Rather, the agreement results from a delicate balance between the dark halo structure, the fraction of baryons collected into each galaxy, and the dynamical response of the dark halo to the assembly of the luminous component.

Massive halos are significantly less efficient at assembling baryons into galaxies than their low-mass counterparts, a trend that agrees with expectations from theoretical models where the mass of the central galaxy is determined by the efficiency of gas cooling. As a result of the structural similarity of dark halos, systems that collect a large fraction of available baryons into a central galaxy have their rotation speeds increased substantially over and above the circular velocity of their surrounding halos. The combined effect leads, for Cold Dark Matter halos, to a direct scaling between disk mass and rotation speed, $M_{\text{disk}} \propto V_{\text{rot}}^3$, which, for approximately constant stellar I -band mass-to-light ratio, is in very good agree-

ment with the observed slope of the I -band Tully-Fisher relation.

The scatter in the numerical Tully-Fisher relation (~ 0.25 mag rms, see lower left panel in Figure 5) is substantially smaller than observed, a somewhat surprising result given the sizeable dispersions in disk mass-to-light ratios and disk mass fractions, as well as in the ratios between disk rotation speed and halo circular velocity observed in our numerical simulations. The small scatter is mainly due to the fact that, although disk mass fractions may vary widely from galaxy to galaxy, these variations are strongly correlated with variations in the disk rotation speed. Model galaxies therefore scatter *along* the Tully-Fisher relation, minimizing the resulting scatter (Figure 7). This is again a non-trivial result stemming from the detailed dark halo structure and from its response to the assembly of the luminous component of the galaxy.

Does the agreement extend to passbands other than I ? Since our galaxy models have approximately constant mass-to-light ratio in the I -band, the simulated slope will be approximately similar in all passbands where mass approximately traces light, such as in the infrared K band. This is consistent with the results of Verheijen (1997), who find a slope of -7.0 in the I -band and of -7.9 in K , when his *complete* sample of galaxies is analyzed. The K -band slope is significantly steeper than the I -band's (-10.4 in K versus -8.7 in I) only when a *restricted* sample with favorable inclination, smooth morphology, steep HI profile edges, and free from bars is considered. The strong dependence on sample selection reflects the large uncertainties in the numerical values of the slope that result from the small dynamic range in velocity (less than a factor of ~ 3 typically) covered by existing Tully-Fisher samples. Taking this into account, and considering that the selection criteria of Verheijen's *complete* sample is closer to those in our analysis (§3.4), we conclude that our models are generally consistent with the slopes of the I and K band Tully-Fisher relations.

The Tully-Fisher relation is also known to be significantly shallower in bluer passbands (see, e.g., Verheijen 1997) a result that can be traced to systematic variations in the mass-to-light ratios as a function of disk rotation speed. Qualitatively our simulations can reproduce the trend, although it is quantitatively much weaker than observed (SN1). This is because fewer stars are formed late in our models than implied by observations (SN3). This effect may have led us to underestimate the scatter in Υ_I . However, considering that the measured scatter is *much* smaller than the observed one, we still consider our conclusion that slope and scatter are consistent with observations to be very solid.

In contrast with this success, we find that the zero-point of the numerical Tully-Fisher relation is offset by about ~ 2 (~ 1.25) magnitudes relative to observations for galaxies formed in the Λ CDM (ACDM) scenario. The offset can be traced to the high-central concentration of dark matter halos formed in these cosmogonies and, to a lesser extent, to the relatively high stellar mass-to-light ratios found in our numerical models ($\Upsilon_I \approx 2.5$). The “concentrations” of dark matter halos would have to be reduced by a factor of ~ 3 -5 or, alternatively, Υ_I would have to be reduced to values as low as ~ 0.4 -0.5 in order to restore agreement with the observed zero-point. As discussed by NS2, neither al-

ternative is quite palatable, since they involve substantial modifications either to the underlying cosmological model, to our understanding of the spectrophotometric evolution of stars, or to our assumptions about the initial stellar mass function. Furthermore, mass-to-light ratios as low as that would exacerbate the problem posed by the small fraction of mass and the large fraction of angular momentum collected by the central disk in low-density universes (see §2.2 and Figure 4).

Including the energetic feedback from evolving stars and supernovae does not improve substantially the agreement between the properties of model galaxies and observation. This is because, in order to fit the empirical correlation linking star formation rate to gas surface density, our feedback model is only efficient in low-mass systems with circular velocities below ~ 100 km s $^{-1}$. The progenitors of massive spirals typically exceed the threshold circular velocity at high redshift, leading to efficient gas cooling and to early onset of star formation. The effects of the kinetic feedback implementation on the Tully-Fisher relation are therefore minor, and only noticeable in systems with low circular velocities. The zero-point disagreement actually worsens at the faint end as star formation is slowed down, affecting the absolute magnitudes of model galaxies more than their rotation speeds. The limited impact of our feedback algorithm also implies that the luminous component of model galaxies is assembled through a sequence of mergers, accompanied by a substantial loss of its angular momentum to the surrounding dark matter. The angular momentum of model galaxies is, as a consequence, about one order of magnitude less than that of observed spirals, in agreement with previous work (cf. NS97).

6. CONCLUDING REMARKS

The results we discuss here illustrate the difficulties faced by hierarchical models that envision the formation of disk galaxies as the final outcome of a sequence of merger events. Agreement with observations appears to require two major modifications to our modeling. (i) Dark halos that are much less centrally concentrated than those formed in the two Cold Dark Matter scenarios we explore here. (ii) Feedback effects dramatically stronger than assumed here, affecting substantially the cooling, accretion, and star formation properties of dark halos perhaps as massive as $V_\Delta \sim 200$ -300 km s $^{-1}$.

The extreme feedback mechanism apparently required to bring the mass and angular momentum of disk galaxies in accordance with hierarchical galaxy formation models should have major implications on further observational clues and traces of the galaxy formation process. Given the paucity of present-day examples of this process at work (Martin 1999), we are led to speculate that star formation (and therefore feedback) episodes were much more violent in the past than in the local universe, perhaps as a result of the lower angular momenta and increased surface density of star forming regions at high redshift. Large scale winds driven by early starbursts, perhaps associated with the formation of stellar spheroids, may rid sites of galaxy formation of early-accreting, low-angular momentum baryons altogether, allowing higher-than-average angular momentum material to collapse later into the modestly star-forming, extended disks prevalent in the local universe.

It remains to be seen whether such scenario for the assembly and transformation of baryons into galaxies withstands observational scrutiny, but so far the $z \sim 3$ evidence being gathered from “Ly-break” galaxies seems to point to a past where starbursts may have been the norm rather than the exception (Heckmann 1999). Resolving the puzzle created by disk galaxy scaling laws has thus the potential to unravel questions of fundamental importance to our understanding of the assembly and evolution of galaxies in a cosmological context.

This work has been supported by the National Aeronau-

tics and Space Administration under NASA grant NAG 5-7151 and by NSERC Research Grant 203263-98. MS and JFN are supported in part by fellowships from the Alfred P. Sloan Foundation. MS is supported in part by fellowship from the David & Lucile Packard foundation. We thank Stephane Courteau, Riccardo Giovanelli and the MarkIII collaboration for making their data available in electronic form, and Cedric Lacey for making available his compilation of the Mathewson et al. data. JFN acknowledges enlightening discussions with Carlos Frenk and Simon White.

REFERENCES

- Barnes, J., Efstathiou, G., 1987, ApJ, 319, 575
 Cole, S.M., Aragón-Salamanca, A., Frenk, C.S., Navarro, J.F., & Zepf, S.E. 1994, MNRAS, 271, 781
 Cole S., & Lacey C. 1996, MNRAS, 281, 716
 Courteau, S. 1997, AJ, 114, 2402
 Contardo, G., Steinmetz, M., & Fritze-von Alvensleben, U. 1998, ApJ, 407, 497
 Dalcanton, J.J., Spergel, D.N., Summers, F.J. 1997, ApJ, 482, 659
 Eisenstein, D.J., Loeb, A., 1996 ApJ, 459, 432
 Eke, V., Cole, S., Frenk, C.S. 1996, MNRAS, 282, 263
 Eke, V., Navarro, J.F., Frenk, C.S. 1998, ApJ, 503, 569
 Elizondo, D., Yepes, G., Kates, R., Müller, V., Klypin, A. 1999, ApJ, 515, 525
 Evrard, A.E., Summers, F.J., & Davis, M. 1994, ApJ, 422, 11
 Giovanelli, R., Haynes, M.P., Herter, T., & Vogt, N.P. 1997, AJ, 113, 22
 Han, M., & Mould, J.R. 1992, ApJ, 396, 453
 Heckman, T.M., 1999, Proceedings of the Royal Society meeting on “The Formation of Galaxies” (astro-ph/9912029).
 Huss A., Jain B., Steinmetz M., 1999a, ApJ, 517, 64
 Huss A., Jain B., Steinmetz M., 1999b, MNRAS, 308, 1011
 Katz, N. 1992, ApJ, 391, 502
 Kauffmann, G., White, S.D.M., Guiderdoni, B. 1993, MNRAS, 264, 201
 Kennicutt, R.C. 1998, ARA&A, 36, 189
 Martin, C.L. 1999, ApJ, 513, 156
 Mathewson, D.S., Ford, V.L., & Buchhorn, M. 1992, ApJS, 81, 413
 Mo, H.J., Mao, S., White, S.D.M. 1998, MNRAS, 295, 319
 Navarro, J.F., Benz, W., 1991, ApJ, 380, 320
 Navarro, J.F., Frenk, C.S., White, S.D.M. 1995, MNRAS, 275, 56
 Navarro, J.F., Frenk, C.S., White, S.D.M. 1996, ApJ, 462, 563 (NFW96)
 Navarro, J.F., Frenk, C.S., White, S.D.M. 1997, ApJ, 490, 493 (NFW97)
 Navarro, J.F., Steinmetz, M. 1997, ApJ, 478, 13 (NS97)
 Navarro, J.F., Steinmetz, M. 2000, ApJ, in press (NS2)
 Navarro, J.F., White, S.D.M. 1993, MNRAS, 265, 271
 Peebles, P.J.E., 1969, ApJ, 155, 393
 Schramm, D.N., Turner, M.S. 1998, Rev.Mod.Ph. 70, 303
 Steinmetz, M. 1996, MNRAS, 278, 1005
 Steinmetz, M., Bartelmann, M. 1995, MNRAS, 272, 570
 Steinmetz, M., Müller, E. 1994, A&A, 281, L97
 Steinmetz, M., Müller, E. 1995, MNRAS, 276, 549
 Steinmetz, M., Navarro, J.F. 1999, ApJ, 513, 555 (SN1)
 Steinmetz, M., Navarro, J.F. 2000, in preparation (SN3)
 Steinmetz, M., White, S.D.M. 1997, MNRAS, 288, 545
 Thornton, K., Gaudlitz, M., Janka, H.-T., Steinmetz, M. 1998, ApJ, 500, 95
 Tissera, P.B., Lambas, D.G., & Abadi, M.G. 1997, MNRAS, 286, 384
 Tormen, G., Bouchet, F.R., White, S.D.M., 1997, MNRAS, 286, 865
 van den Bosch, F.C. 1999, ApJ, in press
 Verheijen, M.A.W., 1997, *PhD thesis*, University of Groningen
 Weil, M., Eke, V.R., Efstathiou, G.P. 1998, MNRAS, 300, 773
 White, S.D.M. 1984, ApJ, 286, 38
 White, S.D.M. 1996, in *Cosmology and Large Scale Structure*, Les Houches session LX, eds. Schaeffer, R., Silk, J., Spiro, M., Zinn-Justin, J., North-Holland, Amsterdam
 White, S.D.M., Frenk, C.S. 1991, ApJ, 379, 25
 White, S.D.M., Rees, M.J. 1978, MNRAS, 183, 341
 White S. D. M., Navarro J. F., Evrard A. E., & Frenk C. S. 1993, Nat, 366, 429
 Willick, J.A., Courteau, S., Faber, S.M., Burstein, D., Dekel, A., & Strauss, M.A. 1997, ApJS, 109, 333